

Combined determination analysis of surface properties evolution towards bentonite by pH treatments

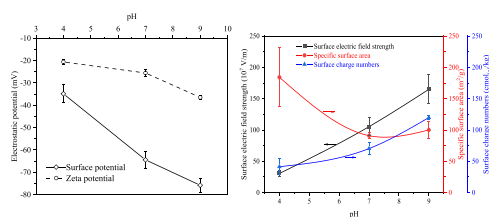
Wei Du^{a,b,c}, Yajun Yang^b, Liang Hu^b, Bokun Chang^b, Gang Cao^b, Mubasher Nasir^{b,c}, Jialong Lv^{b,c,*}

^a State Key Laboratory of Soil Erosion and Dryland Farming on Loess Plateau, Institute of Soil and Water Conservation, Northwest A&F University, Yangling, Shaanxi 712100, China

^b College of Natural Resources and Environment, Northwest A&F University, Yangling 712100, China

^c Key Laboratory of Plant Nutrition and the Agri-environment in Northwest China, Ministry of Agriculture, China

GRAPHICAL ABSTRACT



ARTICLE INFO

Keywords:

Charged clay surface
Surface charge properties
Ion exchange
Protonation
Dissolution

ABSTRACT

Bentonite possesses multiple physicochemical properties because of a large number of charges on the surface. Understanding charges-related surface characteristics at various aqueous solution conditions is critical for bentonite application in various fields, including material modification and environmental restoration. In this study, the evolution of surface properties (surface potential, surface electric field strength, specific surface area, and surface charge numbers) for bentonite samples was investigated using simple ion-exchange experiments and extended combined determination method at different pH conditions. Zeta potential, X-ray diffraction (XRD), and attenuated total reflectance-Fourier transform infrared spectroscopy (ATR-FTIR) techniques were used to examine changes in bentonite structure and surface functional groups. The results demonstrated that surface potential was considerably negative (larger in absolute value) and more sensitive to pH variation than the zeta potential of bentonite under identical conditions. At multiple pH settings, the surface electric field strength and the numbers of bentonite's surface charges were inversely proportional to hydrogen ion concentrations. Cations covalently bonded to clay's surface might reduce negative surface charges and diminish surface electric field strength, particularly as ionic strength increased. Although moderate pH variation has no discernible effect on bentonite interlayer structural alterations, moderate clay dissolution and changes in mineralogical properties may increase the specific surface area of bentonite, particularly when the solvent chemical conditions are acidic. This study comprehensively sheds light on the evolution of surface properties of bentonite clay under acidic, neutral and alkaline conditions, which is helpful in understanding and optimizing its surface performance for material and environmental applications.

* Corresponding author at: College of Natural Resources and Environment, Northwest A&F University, Yangling 712100, China.

E-mail address: ljl@nwsuaf.edu.cn (J. Lv).

<https://doi.org/10.1016/j.colsurfa.2021.127067>

Received 30 April 2021; Received in revised form 18 June 2021; Accepted 21 June 2021

Available online 24 June 2021

0927-7757/© 2021 Elsevier B.V. All rights reserved.

1. Introduction

Bentonite is a type of multipurpose swelling clay that is primarily composed of montmorillonite. Surface area and surface functional groups mutually govern its effectiveness in catalytic reactions and sorption and hence play an important role in industrial dye bleaching [1], catalytic engineering [2], and environmental remediation [3,4]. Because series surface-charges-related properties (charge type, amount, and density) are important parameters to reckon interaction processes closely related to those physicochemical reactions, the surface of bentonite clay can be considered as the central zone of adsorption and catalytic reactions [5,6]. Heavy metals, radionuclides, and organic pollutants in the aquatic environment could be effectively removed via electrostatic and/or non-electrostatic interactions with a charged bentonite clay [7–9]; the amount of catalytically active ion loaded in interlayer space through ion exchange is mainly dependent on layer charge density [10]. Hence, exploring the surface-charge properties of the bentonite clay mineral has far-reaching implications for promoting its use in both industrial and environmental fields.

The pH of the surrounding environment has considerable impact on the charged clay surface properties. The protonation of surface/interlayer functional groups, the formation of complex pore configuration, and the disintegration of a crystalline structure when hydrogen ion concentration changes could dramatically affect the specific surface of bentonite [11]. The pH-dependent charges from clay mineral edges and the heterogeneity of mineral composition were observed to increase the zeta potential of bentonite particles as the pH value increased [5]. The cation exchange capacity of bentonite particles is closely related to their variable charge and chemical compositions. One of the critical regulatory factors is the pH of the surrounding environment [12]. Clay mineral's surface electrostatic fields could polarize molecules and ions, changing their reactivity at the solid–liquid interface [13–15]. The efficiency of which could be profoundly affected by hydrogen-ion concentration. The study progress demonstrated that the charge-related surface properties of clay minerals are susceptible to variation in the surrounding pH, which will inevitably affect clay mineral performance.

In recent years, several methods for determining the surface properties of clay minerals have been proposed. For example, nitrogen adsorption with the Brunauer–Emmett–Teller (BET) method is a common method for measuring the specific surface area of clay minerals [16]. However, gases cannot penetrate the interlayer surfaces, resulting in an underestimation of the material's specific area [17]. Liquid adsorption methods, such as ethylene glycol and ethylene glycol monoethyl ether [18], extensively recognized and used to determine specific surface area; however, many limitations to their use exist, such as time-consuming measurement process and environmental disposal concern [17,19]. Importantly, the results of different measurements may be inconsistent for the given clay minerals [20]. Although advanced techniques such as X-ray photoelectron spectroscopy (XPS) [21] and atomic force microscopy (AFM) [22] have been successfully used to measure the surface potential of materials, strict test conditions and operation technology are required. Furthermore, for many cases, multi-parameter characterization of the research object's surface properties is required to understand the research object [23,24].

Ion exchange at the solid–liquid interface is a fundamental physicochemical reaction that is considerably influenced by the surface charge properties of solid particles; however, ion-exchange reactions can completely reflect the properties of charged surface. Consequently, the ion could be considered as a probe for examining charges-related surface properties of clay minerals. The combined determination of surface properties of charged particles has recently been well established theoretically [25], based on the modified Poisson–Boltzmann equation. By processing experimental results of simple ion exchange, the parameters of surface potential, surface electric field, specific surface area, and numbers of surface charges could be easily and simultaneously computed, and the mathematical relationships among them have been

established [23,24,26]. Actually, relationships between surface properties such as zeta potential and surface potential is well documented in the modified Poisson–Boltzmann equation [27], density functional theory [28,29], and integral equations [30]. For examining interface reactions in aqueous solutions, the simultaneous measurement of multiple parameters for the charged surface under identical conditions is critical [31]. However, previous studies using combined determination obtained surface charge properties at the pH of an aqueous solution in a relatively ideal neutral condition, leaving the applicability of the combined determination method and response of measurement results to acidic or alkaline conditions unrevealed [23,24,26].

Bentonite as a polyfunctional clay mineral that is extensively used in industrial and agricultural production. It is important to uncover its surface charge properties and response mechanism at multiple pH levels. For this reason, the purpose of this research is to: (1) measure the surface charge properties of bentonite using an extended combined determination method, (2) clarify the evolution principle of surface properties at different pH conditions, and (3) analyze and explain the response mechanism of bentonite surface charge properties to pH variation.

2. Materials and method

2.1. Sample preparation

Bentonite was obtained from Henan Jinyuan Environmental Protection Technology Co., Ltd, China. To purify the sample surface, 50 g raw bentonite sample was mixed with 0.1 mol/L HCl solution (1000 ml) in 2 L glass beaker, stirring (600 rpm, 12 h), centrifuging (5000 rpm, 10 min) and discarding the supernatant, the retreatment of precipitate was performed with identical concentration and volume of HCl solution three times in total. HCl solution was subsequently replaced by distilled water and carried out the above process in three repetitions. Then, H⁺-saturated precipitate sample was dried (60 °C), grounded, and sieved through the 60 meshes. All chemicals including HCl and NaOH, were analytical reagents and purchased from Xilong Science Co., Ltd., China.

To investigate the response of bentonite clay surface electrochemical properties towards moderate pH variation, an electrolyte solution with pH values of 4, 7, and 9 were prepared by using HCl or NaOH for pH adjustment. 15 g H⁺-saturated bentonite sample was evenly divided into three parts, and each part was immersed in a 100 ml plastic centrifuge tube containing 50 ml electrolyte with given pH and shaken continuously at 200 rpm for 6 h. After the pH was adjusted to the specified value (4, 7, and 9) with 1 mol/L HCl and/or NaOH, the suspension was centrifuged (5000 rpm, 10 min), dried (60 °C) and ground for XRD and ATR-FTIR analysis. For zeta potential analysis, another 3 g H⁺-saturated bentonite sample was taken and divided into three parts evenly. After mixing with 100 ml CaCl₂/NaCl mixture of 0.1 mol/L separately, the mass concentration of the bentonite suspension was diluted to 100 mg/L. The suspension was sonicated for 10 min, and it was finally adjusted to specific pH for measuring the zeta potential.

2.2. Characterization of bentonite

The zeta potential of bentonite clay was determined with ZetaPlus analyzer (Brookhaven instruments corporation, USA). Mineralogy related analysis of bentonite at different pH was analyzed using XRD (D8 Advance, Bruker, Germany) with CuK α radiation ($\lambda=0.1541$ nm). The running voltage and current were set at 40 kV and 40 mA, respectively, the sweep range of 2θ was 1–60°, and the 2θ -scanning rate was 5 min⁻¹. Patterns were identified by reference to the ICDD-PDF2 2004 database; The surface functional groups information were obtained by determining the vibration spectra of chemical bonds with ATR-FTIR at a spectrum of 4000–400 cm⁻¹ with a resolution of 4 cm⁻¹, which adopted with Nicolet iS10 form Thermo Fisher Scientific company of USA.

The combined determination method [25,31] is a systematic research paradigm to investigate the surface properties of charged

particles. The key parameters such as surface potential, surface electric field strength, etc., could be easily and concurrently obtained by simple ion exchange experiment (e.g., $\text{Na}^+/\text{Ca}^{2+}$ ion-exchange reaction). Briefly, 15 g H^+ -saturated bentonite sample was accurately weighed and equally divided into three parts, then 40 ml of 0.1 mol/L $\text{Ca}(\text{OH})_2/\text{NaOH}$ mixed electrolyte was respectively mixed with 5 g H^+ -saturated sample in 100 ml centrifuge tube. After continuous shaking at constant temperature (25 °C) for 24 h, a certain amount of 0.1 mol/L $\text{Ca}(\text{OH})_2/\text{NaOH}$ electrolyte or H^+ -saturated samples were added to adjust the pH of the suspension to 4, 7 and 9, respectively. Subsequently, 1 mol/L HCl and/or NaOH was used to adjust the pH of suspension until it stabilized at the setting pH after 12 h of shaking. The parameters of surface property can be obtained through the calculation of solid and liquid phase partitioning of $\text{Ca}^{2+}/\text{Na}^+$ at adsorption equilibrium. Because the Ca^{2+} in the high pH solution may include hydroxyl calcium, which will further influence the determination of surface properties, thus the Visual MINTEQ 3.1 was adopted to simulate the concentration of hydroxyl calcium under different pH setting conditions at 25 °C. The simulation results indicated that the concentration of hydroxyl calcium at pH values of 4, 7 and 9 were only 8.0464×10^{-11} , 8.0467×10^{-8} and 8.0461×10^{-6} mol L^{-1} respectively, therefore in measurement the effect of hydroxyl calcium formation on bentonite surface properties could be leaved out. Certainly, if the pH value reaches or exceeds 12.2, the concentration of hydroxyl calcium will be in the same order of magnitude as calcium ion concentration, which will influence the determination of surface properties of bentonite. The mathematical formulas used for the analysis of surface property parameters of bentonite samples at different pH settings are given below:

$$\varphi_0 = \frac{2RT}{(2\gamma_{\text{Ca}} - \gamma_{\text{Na}})F} \ln \frac{a_{\text{Ca}}^0 N_{\text{Na}}}{a_{\text{Na}}^0 N_{\text{Ca}}} \quad (1)$$

$$E_0 = \frac{4\pi}{\epsilon} \text{sgn}(\varphi_0) \sqrt{\frac{\epsilon RT}{2\pi} \left(a_{\text{Na}}^0 \exp\left(-\frac{\gamma_{\text{Na}} F \varphi_0}{RT}\right) + a_{\text{Ca}}^0 \exp\left(-\frac{2\gamma_{\text{Ca}} F \varphi_0}{RT}\right) \right)} \quad (2)$$

$$\text{SSA} = \frac{N_{\text{Na}} \kappa}{m a_{\text{Na}}^0} \exp\left(\frac{\gamma_{\text{Na}} F \varphi_0}{2RT}\right) = \frac{N_{\text{Ca}} \kappa}{m a_{\text{Ca}}^0} \exp\left(\frac{\gamma_{\text{Ca}} F \varphi_0}{2RT}\right) \quad (3)$$

$$\text{SCN} = \frac{10^5 E_0 \epsilon \text{SSA}}{4\pi F} \quad (4)$$

$$\text{where } \gamma_{\text{Ca}} = -0.0213 \ln \sqrt{I} + 1.2331$$

$$\gamma_{\text{Na}} = 0.0213 \ln \sqrt{I} + 0.7669$$

$$\kappa = \sqrt{8\pi F^2 I / \epsilon RT}$$

$$m = 0.5259 \ln(f_{\text{Na}}^0 + f_{\text{H}}^0 / f_{\text{Ca}}^0) + 1.992$$

where φ_0 (mV) is the surface potential of bentonite sample; R (J/K mol), T (K) and F (C/mol) are ideal gas constant, thermodynamic temperature, and Faraday constant respectively; γ_{Na} and γ_{Ca} correspondingly represent the charge correction factor of Na^+ and Ca^{2+} in $\text{Na}^+/\text{Ca}^{2+}$ ion exchange that is influenced by electric field arising from surface charges; a_{Na}^0 (mol/L) and a_{Ca}^0 (mol/L) are the activities of Na^+ and Ca^{2+} in bulk solution at equilibrium; N_{Na} (mol/g) and N_{Ca} (mol/g) are the amounts of adsorbed Na^+ and Ca^{2+} at the charged surface of bentonite; ϵ is the dielectric constant for water ($8.9 \times 10^{-9} \text{ C}^2/\text{J m}$); π is the circumference ratio; E_0 (V/m) is the electrostatic field strength at bentonite surface; SSA (m^2/g) is the specific surface area of bentonite; κ (dm^{-1}) is the Debye-Huckel parameter; SCN ($\text{cmol}_{(\text{c})}/\text{kg}$) is the surface charge numbers of bentonite; I (mol/L) is the ionic strength; f_{Na}^0 (mol/L), f_{H}^0 (mol/L) and f_{Ca}^0 (mol/L) are the equilibrium concentration of Na^+ , H^+ and Ca^{2+} in bulk solution respectively.

3. Results and discussion

3.1. Response of bentonite interlayer structure to pH change

The principal compositions of bentonite at multiple pH levels were analyzed by using X-ray diffraction, Fig. 1 shows the resulting XRD pattern. The sample's characteristics show that bentonite is primarily composed of montmorillonite (PDF 13-0135) and is partially composed of cristobalite (PDF 75-0923) and calcite (PDF 72-1650). The d -spacing of 001 basal planes for montmorillonite at pH values of 4, 7, and 9 was 15.0304, 14.9280, and 15.0309 Å, respectively, indicating that moderate pH variation in solution results in hardly noticeable interlayer spacing changes of montmorillonite. However, under mild acid-base conditions, the intensity of the diffraction peak is relatively weakened, indicating that the crystal phase was slightly changed, reducing the crystallinity of montmorillonite [32]. The analysis demonstrated that moderate pH variation is incapable of influencing bentonite interlayer structure changes. Consequently, the primary effect of pH change on bentonite is presumably adjusting its surface properties via protonation/deprotonation reactions at active surface sites. These binding sites may become positively charged at low pH because of surface protonation reactions (i.e., $\text{SOH} + \text{H}^+ \rightleftharpoons \text{SOH}_2^+$), and negatively charged at high pH because of surface deprotonation reactions (i.e., $\text{SOH} \rightleftharpoons \text{SO}^- + \text{H}^+$) [33].

3.2. Changes in zeta potential and surface potential

Fig. 2 shows variations in zeta potential and surface potential of bentonite at a moderate pH, which revealed the following similarities and differences. First, all tests demonstrated a negative zeta potential and a surface potential; no isoelectric point or charge reversal is observed, indicating that the surface of the tested bentonite clay is negatively charged, and a constant negative charge induces a significant contribution to the surface potential of bentonite [34]. In reality, it is accepted that the bentonite surface is negatively charged by measuring its zeta potentials over a wide pH range [5,35,36] and that these negative charges are attributed to isomorphic replacement, crystal lattice defects, fragmentary particle edges, and structural hydroxyl groups [37]. However, noted that the measured surface potential values in this study were only -34.84 , -64.43 , and -75.79 mV at pH values of 4, 7, and 9, respectively, which presumably is attributed to the gradual depletion of pH-dependent negative charges on clay edges as pH decreased. Furthermore, the underestimated surface potential should be attributed to the dielectric saturation and polarization of distributed water molecules around the charged clay surface. This is because in the Gouy-Chapman model, the electrostatic field strength at the clay-water

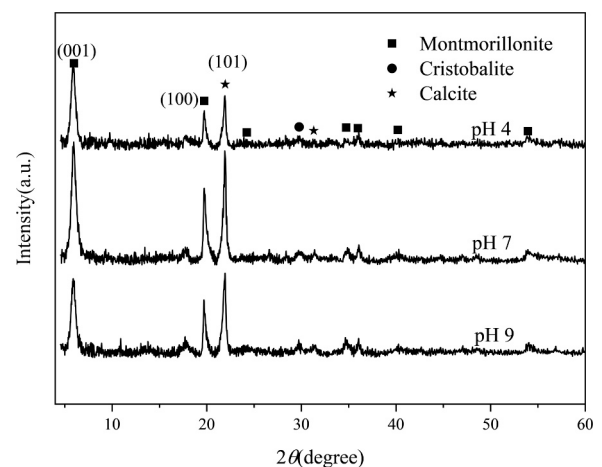


Fig. 1. The XRD patterns of bentonite at different pH.

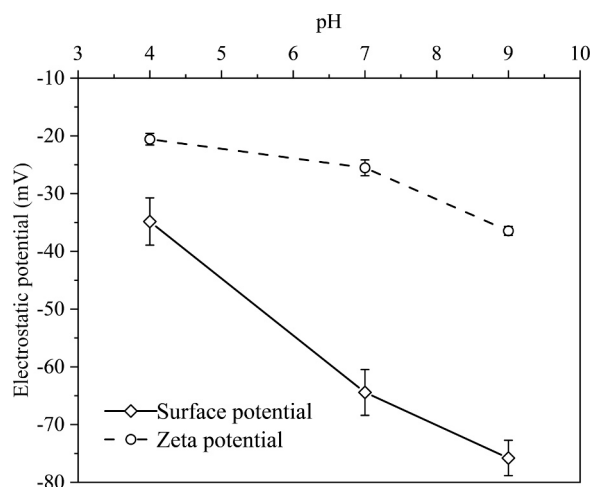


Fig. 2. Surface potential and Zeta potential of bentonite at different pH with identical ionic strength ($I=0.4$ M).

interface is hypothetically underestimated for invariable dielectric constants, and polarization of water molecules could decrease the surface potential [38,39]; Second, negative zeta potential and surface potential progressively decreases as pH decreases, indicating a certain amount of variable charge carried on bentonite surface. Many studies reported that edge-face interactions influence the magnitude of zeta potential in bentonite clay particles as a function of pH [40,41]. In montmorillonite, the silanol groups of tetrahedral sheets and dioctahedral edge aluminol groups could regulate surface electrical properties by participating in chemical reactions in aqueous systems. The surface net negative charge can be reduced by hydroxyl protonation in acidic media with increase via hydroxyl deprotonation in alkaline media [12,42]. Consequently, the changes in zeta potential caused by pH (Fig. 2) can be attributed primarily to protonation/deprotonation reactions of silanol and aluminol groups at the bentonite surface.

Fig. 2 shows the differences between zeta potential and surface potential. At a given pH, the zeta potential was smaller (less negative) than the surface potential. Theoretically, zeta potential is not equivalent to surface potential because the former refers to the potential of the shear plane at a certain distance away from the surface, and such potential exponentially decays with distance [43]. Recently, studies discovered that the zeta potential is several orders of magnitude less than the corresponding surface potential [44,45]. Compared to surface potential, non-significant changes in zeta potential because of pH variations indicate that zeta potential is not pH sensitive [5,46]. Furthermore, discrepancies between them rapidly decreased as pH decreased, indicating that the variation trends for surface potential and zeta potential are qualitatively different. This observation, which is most likely attributed to an increase in counter-ion concentration, will screen the strength of the negative surface electrostatic field and compress the thickness of the electrical double layer [26,47]. Because the adsorbed counter ions compress the electric double layer more than the sliding layer, the surface potential changes more than the zeta potential [44, 48].

3.3. Changes in surface electric field strength, specific surface area, and numbers of surface charges

Other parameters, in addition to surface potential, can be used to characterize the surface electrochemical properties of bentonite as pH changes in a moderate range. Fig. 3 shows the measured surface electric field strength, specific surface area, and surface charge numbers at various pH levels. In a moderate pH range, the surface electric field strength and surface negative charge numbers of bentonite decreased with decrease in pH, whereas the specific surface area increased with

decrease pH. In other words, the former are negatively correlated with the bulk solution's hydrogen ion concentration, whereas the latter is positively correlated with the bulk solution's hydrogen ion concentration. The two observations made above can be theoretically rationalized. As per the classical electric double layer theory, counter ions in aqueous solution would diffusely distribute near charged clay particles because of the combined effects of random thermal motion and electrostatic attraction force because of negative surface charges [49,50]. To our knowledge, the hydrogen ion can reach the Stern layer and interact with charged clay minerals via various mechanisms [45,51,52]. The ion-surface interactions at different pH are determined by the surface-electric-field-dependent coordinate bond between H^+ and O^- ions, or by the electrostatic force between H^+ and negatively charged surface [52]. However, cations covalently bound to the negatively charged surface of clay mineral would inevitably deplete the clay surface negative charges, and this effect would be more noticeable as ionic strength increased [53,54], which is extremely similar to the case of DNA solution [55]. The observed evolution of surface electric field strength and surface negative charge numbers with pH variation is consistent with the theoretical description provided above.

The measured average values of specific surface area for bentonite at pH 4, 7, and 9 were, however, 184.2, 90.91, and 100.0 m^2/g , respectively. Specific surface area at pH 4 and 9 was 2.026 and 1.010 times greater than that at pH 7, respectively, compared to neutral pH conditions. This result indicates that specific surface area increased under moderately acidic and alkaline conditions, with the increase being more noticeable at low pH. In general, the specific surface area of bentonite increases with the hydrogen ions concentration [2,32]. To date, this increase has been attributed to the replacement of interlayer cations with hydrogen ions, and bentonite porosity (micro or mesopores) increased with increasing hydrogen ion concentration [11,56]. Under low or high pH conditions, montmorillonite dissolution and ion leaching from the octahedral and tetrahedral site expose platelet edges of bentonite [32,57]. Because of changes in XRD pattern at different pH (Fig. 1), the increasing specific surface area of bentonite under moderately acidic and alkaline conditions is presumably attributed to the combined effects of protonation, slight dissolution of clay, and a series of changes in mineralogical properties such as void ratio and morphologies.

3.4. Surface functional groups response to pH variation and its relationship to surface charge properties

To examine the effect of pH changes on the functional groups of

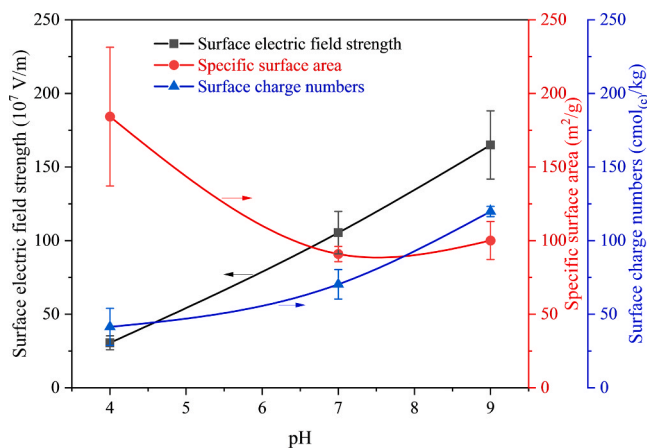


Fig. 3. Trends in bentonite surface electric field strength, specific area, and charge numbers with moderate pH variation (The arrows pointing left or right for the three curves represent the corresponding numbers and units for the curves shown).

bentonite, ATR-FTIR spectra were performed in the spectrum range of 4000–400 cm^{-1} as a common approach for identifying the characteristics of functional groups (Fig. 4).

The absorption band at $\sim 3614 \text{ cm}^{-1}$ was attributed to the stretching OH groups of (Al)O-H or (Mg)O-H bonds [58]. The intensity of stretching bands decreases as pH decreases, confirming that negatively charged OH groups are bound with positively charged ions to bentonite's surface active sites [59]. Spectroscopic results show that as the hydrogen ion concentration in the bulk solution increased, the negative charges on the bentonite surface were depleted, resulting in a gradual decrease in the number of negative charges on the surface and a gradual decrease in electronegativity. The variation of surface electronegativity concerning the aforementioned ATR-FTIR spectra analysis could explain the trends of surface electrochemical parameters with pH changes, such as surface (or zeta) potential (Fig. 2), electric field strength, and negative charge numbers (Fig. 3). The broad vibration band at $\sim 3388 \text{ cm}^{-1}$ was caused by silanol's O-H stretching vibration and adsorbed interlayer water at the silica surface [60]. With decrease in pH, the intensities of stretching bands gradually decreased and shifted from 3388.12 to 3379.24 cm^{-1} , indicating that the O-H of silanol groups and adsorbed interlayer water strongly interacted with permeated hydrogen ions in clay. The deformation vibration intensity of H-O-H for adsorbed water at $\sim 1634 \text{ cm}^{-1}$ [32,61,62] decreased with the decrease of pH, indicating a decrease in water content with increase in hydrogen ion concentration in the bulk solution. This is because when protons permeate into the clay layers and attack the O-H groups, dehydroxylation and dissolution of the structural atoms occur, which can be readily responded to by changes in the characteristic absorption bands, attributed to vibrations in O-H groups [63]. The strong absorption peak observed at $\sim 1005\text{--}1017 \text{ cm}^{-1}$ was attributed to Si-O-Si asymmetric stretching vibrations [64,65]. The band at $\sim 791\text{--}792 \text{ cm}^{-1}$ may be attributed to the presence of cristobalite and low-crystalline silica [33,66,67], the intensity of which decreased with increase in hydrogen ion concentration, most likely because of tetrahedral sheet transformation. The results of the above ATR-FTIR analysis indicate that the amounts of O-H groups for the central atom from tetrahedral/octahedral sheet regulated the pH-dependent negative charges. The surface negative charge amounts of bentonite clay decreased as the surface concentration of hydroxyl ions decreased [68].

4. Conclusions

The evolution of surface electrochemical properties for bentonite samples has been systematically examined using extended combined determination at moderate pH variations, yielding the following conclusions. Firstly, the surface potential was more negative (larger in absolute value) and more sensitive to pH variation than the zeta potential of bentonite. Second, at different pH levels, the surface electric field strength and number of surface charges of bentonite were inversely proportional to the hydrogen ion concentrations. The shielding of positively charged ions to negative surface charges, compression of the electric double layer, and protonation of (Al/Mg) O-H bonds and interlayer Si-OH regulated the changing trend of surface electric field strength and number of surface charges with decrease in pH. Third, while moderate pH variation is incapable of influencing bentonite interlayer structure changes, slight dissolution of clay and changes in mineralogical properties may increase the specific surface area of bentonite, particularly when the solvent chemical conditions are acidic.

CRedit authorship contribution statement

Jialong Lv: Conceptualization, Methodology. **Wei Du:** Data curation, Writing - original draft. **Yajun Yang:** Visualization. **Liang Hu:** Investigation. **Jialong Lv and Gang Cao:** Supervision. **Bokun Chang:** Software, Validation. **Jialong Lv and Mubasher Nasir:** Writing - review & editing.

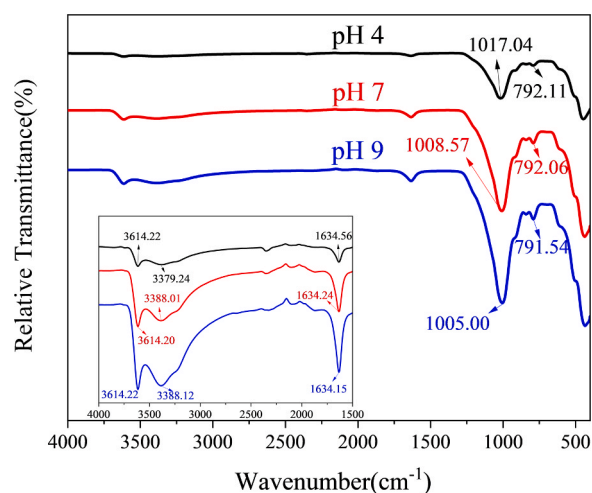


Fig. 4. ATR-FTIR spectra of bentonite at different pH.

Declaration of Competing Interest

The authors declare that they have no known competing financial interests or personal relationships that could have appeared to influence the work reported in this paper.

Acknowledgements

This work was supported by the Doctoral Start-Up Research Fund of Northwest A&F University (2452018041), the Open Fund of State Key Laboratory of Soil Erosion and Dryland Farming on the Loess Plateau (A314021402–1906), and the National Key Research and Development Program of China (No. 2017YFD0200205).

References

- [1] A. Kausar, M. Iqbal, A. Javed, K. Aftab, H.N. Bhatti, S. Nouren, Dyes adsorption using clay and modified clay: a review, *J. Mol. Liq.* 256 (2018) 395–407.
- [2] P. Pushpaaletha, S. Rugmini, M. Lalithambika, Correlation between surface properties and catalytic activity of clay catalysts, *Appl. Clay Sci.* 30 (2005) 141–153.
- [3] S. Gu, X. Kang, L. Wang, E. Lichtfouse, C. Wang, Clay mineral adsorbents for heavy metal removal from wastewater: a review, *Environ. Chem. Lett.* 17 (2019) 629–654.
- [4] S. Kakaei, E.S. Khameneh, F. Rezazadeh, M.H. Hosseini, Heavy metal removing by modified bentonite and study of catalytic activity, *J. Mol. Struct.* 1199 (2020), 126989.
- [5] R. Mészáros, A. Jobbik, G. Varga, S. Bárány, Electrochemical properties of Na-bentonite particles in electrolytes and surfactants solution, *Appl. Clay Sci.* 178 (2019), 105127.
- [6] V. Aghazadeh, S. Barakan, E. Bidari, Determination of surface protonation-deprotonation behavior, surface charge, and total surface site concentration for natural, pillared and porous nano bentonite heterostructure, *J. Mol. Struct.* 1204 (2020), 127570.
- [7] E. Alvarez-Ayuso, A. García-Sánchez, Removal of heavy metals from waste waters by natural and Na-exchanged bentonites, *Clays Clay Miner.* 51 (2003) 475–480.
- [8] E.L. Tran, N. Teutsch, O. Klein-BenDavid, N. Weisbrod, Uranium and cesium sorption to bentonite colloids under carbonate-rich environments: implications for radionuclide transport, *Sci. Total Environ.* 643 (2018) 260–269.
- [9] H. Han, M.K. Rafiq, T. Zhou, R. Xu, O. Mašek, X. Li, A critical review of clay-based composites with enhanced adsorption performance for metal and organic pollutants, *J. Hazard. Mater.* 369 (2019) 780–796.
- [10] C.H. Zhou, An overview on strategies towards clay-based designer catalysts for green and sustainable catalysis, *Appl. Clay Sci.* 53 (2011) 87–96.
- [11] V. Krupskaya, L. Novikova, E. Tyupina, P. Belousov, O. Dorzhieva, S. Zakusin, K. Kim, F. Roessner, E. Badetti, A. Brunelli, The influence of acid modification on the structure of montmorillonites and surface properties of bentonites, *Appl. Clay Sci.* 172 (2019) 1–10.
- [12] S. Kaufhold, R. Dohrmann, The variable charge of dioctahedral smectites, *J. Colloid Interface Sci.* 390 (2013) 225–233.
- [13] C.J. Rhodes, Electric fields in zeolites: fundamental features and environmental implications, *Chem. Pap.* 70 (2016) 4–21.
- [14] W. Du, R. Li, X. Liu, R. Tian, W. Ding, H. Li, Estimating Hofmeister energy in ion-clay mineral interactions from the Gouy-Chapman theory, *Appl. Clay Sci.* 146 (2017) 122–130.

- [15] W. Du, X. Liu, R. Li, R. Tian, W. Ding, H. Li, Theory to describe incomplete ion exchange in charged heterogeneous systems, *J. Soils Sediment.* 19 (2019) 1839–1849.
- [16] S. Kaufhold, R. Dohrmann, M. Klinkenberg, S. Siegesmund, K. Ufer, N₂-BET specific surface area of bentonites, *J. Colloid Interface Sci.* 349 (2010) 275–282.
- [17] K. Pennell, 2.5 specific surface area, *Methods Soil Anal. Part 4 Phys. Methods* 5 (2002) 295–315.
- [18] A.B. Cerato, A.J. Lutenegeger, Determination of surface area of fine-grained soils by the ethylene glycol monoethyl ether (EGME) method, *Geotech. Test. J.* 25 (2002) 315–321.
- [19] M. Knadel, E. Arthur, P. Weber, P. Moldrup, M.H. Greve, Z.P. Chrysodonta, L.W. De Jonge, Soil specific surface area determination by visible near-infrared spectroscopy, *Soil Sci. Soc. Am. J.* 82 (2018) 1046–1056.
- [20] F. Macht, K. Eusterhues, G.J. Pronk, K.U. Totsche, Specific surface area of clay minerals: comparison between atomic force microscopy measurements and bulk-gas (N₂) and-liquid (EGME) adsorption methods, *Appl. Clay Sci.* 53 (2011) 20–26.
- [21] M.A. Brown, Z. Abbas, A. Kleibert, R.G. Green, A. Goel, S. May, T.M. Squires, Determination of surface potential and electrical double-layer structure at the aqueous electrolyte-nanoparticle interface, *Phys. Rev. X* 6 (2016), 011007.
- [22] X. He, X. Liu, D. Song, B. Nie, Effect of microstructure on electrical property of coal surface, *Appl. Surf. Sci.* 483 (2019) 713–720.
- [23] J. Liu, Z. Wang, F. Hu, C. Xu, R. Ma, S. Zhao, Soil organic matter and silt contents determine soil particle surface electrochemical properties across a long-term natural restoration grassland, *CATENA* 190 (2020), 104526.
- [24] S. Xue, W. Ke, F. Zhu, J. Fan, Q. Wang, Z. Liu, W. Hartley, Evaluating aggregate stability, surface properties and disintegration behaviour of bauxite residue induced by Ca/Na, *Land Degrad. Dev.* (2020).
- [25] H. Li, J. Hou, X. Liu, R. Li, H. Zhu, L. Wu, Combined determination of specific surface area and surface charge properties of charged particles from a single experiment, *Soil Sci. Soc. Am. J.* 75 (2011) 2128–2135.
- [26] F. Hu, J. Liu, C. Xu, Z. Wang, G. Liu, H. Li, S. Zhao, Soil internal forces initiate aggregate breakdown and splash erosion, *Geoderma* 320 (2018) 43–51.
- [27] L. Bhuiyan, C. Outhwaite, Thermodynamics and phase separation of a de-ionized colloidal system in the symmetric Poisson–Boltzmann and mean spherical approximation theories, *J. Chem. Phys.* 116 (2002) 2650–2657.
- [28] Y.-X. Yu, J.-Z. Wu, G.-H. Gao, Ionic distribution, electrostatic potential and zeta potential at electrochemical interfaces, *Chin. J. Chem. Eng.* 12 (2004) 688–695.
- [29] K. Wang, Y.-X. Yu, G.-H. Gao, Density functional study on the structural and thermodynamic properties of aqueous DNA-electrolyte solution in the framework of cell model, *J. Chem. Phys.* 128 (2008), 185101.
- [30] Y.-X. Yu, J. Wu, G.-H. Gao, Density-functional theory of spherical electric double layers and ζ potentials of colloidal particles in restricted-primitive-model electrolyte solutions, *J. Chem. Phys.* 120 (2004) 7223–7233.
- [31] X. Liu, H. Li, R. Li, R. Tian, C. Xu, Combined determination of surface properties of nano-colloidal particles through ion selective electrodes with potentiometer, *Analyst* 138 (2013) 1122–1129.
- [32] M. Toor, B. Jin, S. Dai, V. Vimonses, Activating natural bentonite as a cost-effective adsorbent for removal of Congo-red in wastewater, *J. Ind. Eng. Chem.* 21 (2015) 653–661.
- [33] S. Yang, D. Zhao, H. Zhang, S. Lu, L. Chen, X. Yu, Impact of environmental conditions on the sorption behavior of Pb (II) in Na-bentonite suspensions, *J. Hazard. Mater.* 183 (2010) 632–640.
- [34] B.E. Şans, O. Güven, F. Esenli, M.S. Çelik, Contribution of cations and layer charges in the smectite structure on zeta potential of Ca-bentonites, *Appl. Clay Sci.* 143 (2017) 415–421.
- [35] D. Niriella, R. Carnahan, Comparison study of zeta potential values of bentonite in salt solutions, *J. Dispers. Sci. Technol.* 27 (2006) 123–131.
- [36] M.H. Baik, S.Y. Lee, Colloidal stability of bentonite clay considering surface charge properties as a function of pH and ionic strength, *J. Ind. Eng. Chem.* 16 (2010) 837–841.
- [37] A. Chakir, J. Bessiere, K.E. Kacemi, Bb Marouf, A comparative study of the removal of trivalent chromium from aqueous solutions by bentonite and expanded perlite, *J. Hazard. Mater.* 95 (2002) 29–46.
- [38] X. Liu, B. Feng, R. Tian, R. Li, Y. Tang, L. Wu, W. Ding, H. Li, Electrical double layer interactions between soil colloidal particles: polarization of water molecule and counterion, *Geoderma* 380 (2020), 114693.
- [39] X. Liu, R. Tian, W. Du, R. Li, W. Ding, H. Li, A theory to determine the surface potentials of clay particles in electrolyte solutions, *Appl. Clay Sci.* 169 (2019) 112–119.
- [40] G. Lagaly, Principles of flow of kaolin and bentonite dispersions, *Appl. Clay Sci.* 4 (1989) 105–123.
- [41] T. Tulun, N. Gungor, Rheological characteristics of aqueous Ca-bentonite dispersions, *J. Sci. Ind. Res.* 58 (1999) 607–615.
- [42] D. Zhao, S. Feng, C. Chen, S. Chen, D. Xu, X. Wang, Adsorption of thorium (IV) on MX-80 bentonite: effect of pH, ionic strength and temperature, *Appl. Clay Sci.* 41 (2008) 17–23.
- [43] H. Li, S. Wei, C. Qing, J. Yang, Discussion on the position of the shear plane, *J. Colloid Interface Sci.* 258 (2003) 40–44.
- [44] W. Ding, X. Liu, L. Song, Q. Li, Q. Zhu, H. Zhu, F. Hu, Y. Luo, L. Zhu, H. Li, An approach to estimate the position of the shear plane for colloidal particles in an electrophoresis experiment, *Surf. Sci.* 632 (2015) 50–59.
- [45] X. Liu, F. Hu, W. Ding, R. Tian, R. Li, H. Li, A how-to approach for estimation of surface/Stern potentials considering ionic size and polarization, *Analyst* 140 (2015) 7217–7224.
- [46] O. Duman, S. Tunç, Electrokinetic and rheological properties of Na-bentonite in some electrolyte solutions, *Microporous Mesoporous Mater.* 117 (2009) 331–338.
- [47] W. Du, X. Liu, R. Tian, R. Li, W. Ding, H. Li, Specific ion effects of incomplete ion-exchange by electric field-induced ion polarization, *RSC Adv.* 10 (2020) 15190–15198.
- [48] X. Liu, W. Ding, R. Tian, W. Du, H. Li, Position of shear plane at the clay–water interface: strong polarization effects of counterions, *Soil Sci. Soc. Am. J.* 81 (2017) 268–276.
- [49] D.A. Laird, Influence of layer charge on swelling of smectites, *Appl. Clay Sci.* 34 (2006) 74–87.
- [50] Y. Liang, N. Hilal, P. Langston, V. Starov, Interaction forces between colloidal particles in liquid: theory and experiment, *Adv. Colloid Interface Sci.* 134 (2007) 151–166.
- [51] D.F. Parsons, M. Boström, P.L. Nostro, B.W. Ninham, Hofmeister effects: interplay of hydration, nonelectrostatic potentials, and ion size, *Phys. Chem. Chem. Phys.* 13 (2011) 12352–12367.
- [52] D. Liu, W. Du, X. Liu, R. Tian, H. Li, To distinguish electrostatic, coordination bond, nonclassical polarization, and dispersion forces on cation–clay interactions, *J. Phys. Chem. C* 123 (2019) 2157–2164.
- [53] W. Du, R. Li, X.-M. Liu, R. Tian, H. Li, Specific ion effects on ion exchange kinetics in charged clay, *Colloids Surf. A Physicochem. Eng. Asp.* 509 (2016) 427–432.
- [54] W. Hao, S.L. Flynn, T. Kashiwabara, M.S. Alam, S. Bandara, L. Swaren, L. J. Robbins, D.S. Alessi, K.O. Konhauser, The impact of ionic strength on the proton reactivity of clay minerals, *Chem. Geol.* 529 (2019), 119294.
- [55] K. Wang, Y.-X. Yu, G.-H. Gao, G.-S. Luo, Density-functional theory and Monte Carlo simulation study on the electric double layer around DNA in mixed-size counterion systems, *J. Chem. Phys.* 123 (2005), 234904.
- [56] E. González-Pradas, E. Villafranca-Sánchez, M. Villafranca-Sánchez, F. del Rey-Bueno, A. Valverde-García, A. García-Rodríguez, Evolution of surface properties in a bentonite as a function of acid and heat treatments, *J. Chem. Technol. Biotechnol.* 52 (1991) 211–218.
- [57] W.-M. Ye, Z. Zheng, B. Chen, Y.-G. Chen, Y.-J. Cui, J. Wang, Effects of pH and temperature on the swelling pressure and hydraulic conductivity of compacted GMZ01 bentonite, *Appl. Clay Sci.* 101 (2014) 192–198.
- [58] F.E. Soetaredjo, A. Ayucitra, S. Ismadji, A.L. Maukar, KOH/bentonite catalysts for transesterification of palm oil to biodiesel, *Appl. Clay Sci.* 53 (2011) 341–346.
- [59] K. Tohdee, L. Kaewsichan, Potential of BCDMAcI modified bentonite in simultaneous adsorption of heavy metal Ni (II) and humic acid, *J. Environ. Chem. Eng.* 6 (2018) 5616–5624.
- [60] M. Belhadri, A. Mokhtar, S. Meziani, F. Belkhadem, M. Sassi, A. Bengueddach, Novel low-cost adsorbent based on economically modified bentonite for lead (II) removal from aqueous solutions, *Arab. J. Geosci.* 12 (2019) 1–13.
- [61] J. Madejová, M. Janek, P. Komadel, H.-J. Herbert, H. Moog, FTIR analyses of water in MX-80 bentonite compacted from high salinary salt solution systems, *Appl. Clay Sci.* 20 (2002) 255–271.
- [62] S. Ismadji, D.S. Tong, F.E. Soetaredjo, A. Ayucitra, W.H. Yu, C.H. Zhou, Bentonite hydrochar composite for removal of ammonium from Koi fish tank, *Appl. Clay Sci.* 119 (2016) 146–154.
- [63] A.S. Özcan, A. Özcan, Adsorption of acid dyes from aqueous solutions onto acid-activated bentonite, *J. Colloid Interface Sci.* 276 (2004) 39–46.
- [64] J.I. Martínez-Costa, R. Leyva-Ramos, E. Padilla-Ortega, Sorption of diclofenac from aqueous solution on an organobentonite and adsorption of cadmium on organobentonite saturated with diclofenac, *Clays Clay Miner.* 66 (2018) 515–528.
- [65] B. Tanc, N. Orakdogan, A versatile strategy for mechanically durable nanocomposite cryogels based on cationic (alkyl) methacrylates and hydrophilic bentonite via freezing (cryo) polymerization, *Soft Matter* 15 (2019) 3208–3226.
- [66] J. Madejova, P. Komadel, Baseline studies of the clay minerals society source clays: infrared methods, *Clays Clay Miner.* 49 (2001) 410–432.
- [67] J. Temuujin, M. Senna, T. Jadambaa, D. Burmaa, S. Erdenechimeg, K.J. MacKenzie, Characterization and bleaching properties of acid-leached montmorillonite, *J. Chem. Technol. Biotechnol. Int. Res. Process Environ. Clean. Technol.* 81 (2006) 688–693.
- [68] A. Goodarzi, S.N. Fateh, H. Shekary, Impact of organic pollutants on the macro and microstructure responses of Na-bentonite, *Appl. Clay Sci.* 121 (2016) 17–28.